Synthesis and Characterization of CdS Nanoclusters in a Quaternary Microemulsion: the Role of the Cosurfactant

Maria Lucia Curri

CNR CS CFILM, c/o Dipartimento di Chimica, Università degli Studi di Bari, Campus Universitario, Via Orabona 4, I-70026 Bari, Italy

Angela Agostiano,* Liberato Manna, and Mario Della Monica

Dipartimento di Chimica, Università degli Studi di Bari, Campus Universitario, Via Orabona 4, I-70126 Bari, Italy

Massimo Catalano

CNR IME, Via Arnesano I-73100 Lecce, Italy

Luca Chiavarone, Vincenzo Spagnolo, and Mario Lugarà

INFM-Dipartimento Interateneo di Fisica di Bari, Via Orabona 4, I-70126 Bari Italy

Received: February 29, 2000; In Final Form: June 30, 2000

Nanostructured semiconductor particles are currently under intense investigation because of their interesting photophysical and photochemical properties. Several preparation methods have been exploited for this class of materials; among them, the use of reverse micelles or "water-in-oil" microemulsions is a simple and successful preparative route. In this paper, a novel synthetic medium has been exploited, consisting of a quaternary CTAB/*n*-pentanol/*n*-hexane/water microemulsion. The presence of cosurfactant (*n*-pentanol), in addition to water, allows the simultaneous modulation of the water droplets dimensions and their exchange dynamics. Nanoparticles were characterized by UV−vis and photoluminescence spectroscopy, High-Resolution Transmission Electron Microscopy, and Raman spectroscopy. All measurements showed that the mean size of the nanoparticles is governed by the pentanol content of the system. They also possess a narrow size distribution and a good degree of crystallinity. Moreover, pentanol has an influence on the stability of CdS clusters, behaving as a capping agent at high concentrations. Stopped-flow measurements elucidated the influence of the cosurfactant in the kinetics of nucleation and growth.

Introduction

The study of the physical and chemical properties of nanometer sized semiconductor clusters has been an active field of research for more than a decade. This class of materials not only provides many new opportunities for understanding the underlying physics at reduced dimensions but will be useful for technological applications in chemical processes,[1−6] in biology[7,8] and in the area of optical and optoelectronic devices.[9−11]

The main issue in the preparation of semiconductor nanocrystals is a careful control of semiconductor size and, even more important, of their size distribution. Moreover, their subsequent manipulation requires an efficient procedure of recovery and stabilization. Among the several preparations proposed in the literature[12−15] a popular method makes use of reverse micelles or "water-in-oil" microemulsions. Reverse micelles are suitable reaction media for the synthesis of nanoparticles because water droplets can be seen as nanoreactors, favoring the formation of small crystallites with a sufficiently narrow size distribution.[16−21] This technique often yields particles with a good crystallinity without high temperature requirements and can be used to synthesize several classes of nanocrystals. Stabilization and recovery of the particles can be achieved by capping their surface with various organic molecules immediately after the synthesis.[22−25]

In this paper, a novel synthetic medium has been exploited: the four components CTAB/*n*-pentanol/*n*-hexane/water system. We studied in detail the role of the cosurfactant (*n*-pentanol) as a potentially useful parameter in regulating the size and the stability of CdS clusters.

The composition of the four-component microemulsion is completely defined by three parameters: the surfactant molar concentration ([CTAB]), the molar ratio between water and surfactant (W_0), and the molar ratio between alcohol (*n*-pentanol) and surfactant (P_0). CTAB has a low solubility in *n*-hexane/*n*-pentanol; a higher solubility is achieved when aggregates with a small amount of water ($W_0 = 5$) are formed.[26] Systems at different W_0 (>5) can be prepared by water (or aqueous salt solution) dilution of a stock solution prepared at $W_0 = 5$ and at a given P_0. At the composition used in the present study ([CTAB] ≈ 0.1 M, $P_0 = 8-20$ and W_0 up to 80) the CTAB/pentanol/*n*-hexane/water microemulsion forms L_2 region, i.e., a liquid isotropic phase formed by disconnected aqueous domains dispersed in a continuous organic bulk.[26] The nearly

* To whom correspondence should be addressed. E-mail: agostiano@area.ba.cnr.it Tel: +39 080 5442060. Fax: +39 080 5442128

10.1021/jp0007639 CCC: $19.00
Published on Web 08/09/2000

spherical droplets are stabilized by a surfactant/cosurfactant interfacial film. At higher water contents ($W_0 > 80$), a phase separation occurs, resulting in a aqueous phase and a microemulsion phase (Winsor II system). In this system, it is possible to modulate the water droplets dimension and surface dynamics by either varying the water or the alcohol content.[27] In fact, the alcohol has two effects on the interfacial properties of the microemulsion:

(a) The microstructural effect. The alcohol absorbs to the interfacial film and thus modifies the surfactant packing parameters. This, in turn, influences the radius of curvature of the microemulsion droplet. It should be noted that this effect is of particular relevance in the system under study; the CTAB cannot form reverse micelles in *n*-hexane without the assistance of pentanol, due to its unfavorable packing parameter.

(b) The dynamic effect. A minimum quantity of cosurfactant is sometimes required for the existence of stable water in oil microemulsions (as in our case). Nevertheless, droplets formed in these conditions do not show the same interface rigidity observed in ternary microemulsions, where the plain presence of the surfactant makes the interfacial film more compact. Experimental evidence shows that the addition of cosurfactants to ternary, stable, microemulsive systems decreases the interface organization by affecting the compactness of the film and its temporal stability; surfactants continuously migrate between the interface and the bulk organic phase. When alcohols are used as cosurfactants, the interface stability is inversely proportional to the alcohol alkyl chain. The exact dependence varies from system to system, but pentanol usually ranks as a strong interface de-stabilizer. In this physically "frustrated" configuration the droplets tend to increase their interaction with the external environment and, ultimately, their exchange dynamics.

Material and Methods

Cetyltrimethylammonium bromide (CTAB) and sodium bis-(2−ethylhexil)sulfosuccinate (AOT), *n*-hexane, *n*-pentanol, thiophenol, dodecanethiol, pyridin, methanol, and ethanol were obtained from Fluka. Cadmium nitrate and sodium sulfide were purchased from Aldrich. All of the chemicals were used without any further purification. Double-distilled water in an all-quartz apparatus ($\chi < 1.3 \times 10^{-4}$ Sm^{1-}) was used.

UV−vis absorption spectra were recorded using a UVIKON 942 Kontron UV−vis spectrophotometer. The position of the absorption maximum was correlated to the particles mean radius by using well-known relations.[27]

TEM observations were performed by using a JEOL 4000 EX II transmission electron microscope, operating at 400 kV accelerating voltage, with an interpretable resolution limit of 0.16 nm. CdS nanoparticles were extracted from the microemulsion and redispersed in ethanol according to the procedure described later in the paper. A small drop of the solution was then dropped onto a carbon coated copper grids, allowing the alcohol to evaporate. Both bright field (BF), high resolution (HREM), and selected area diffraction patterns (SADP) were obtained in order to evaluate the particle shape, crystal structure, and diameter distribution.

Raman backscattering was excited at room temperature on CdS nanocrystals semiconductor extracted from microemulsion and cast on a glass slide. Several Ar^+ and Kr^+ lines were used as the exciting source. The scattered light was analyzed by a Jobin−Yvon T64000 triple spectrometer with a focal length of 0.64 m, equipped with a liquid N_2-cooled CCD system. The slits were set for a spectral resolution of 0.6 cm^{-1}.

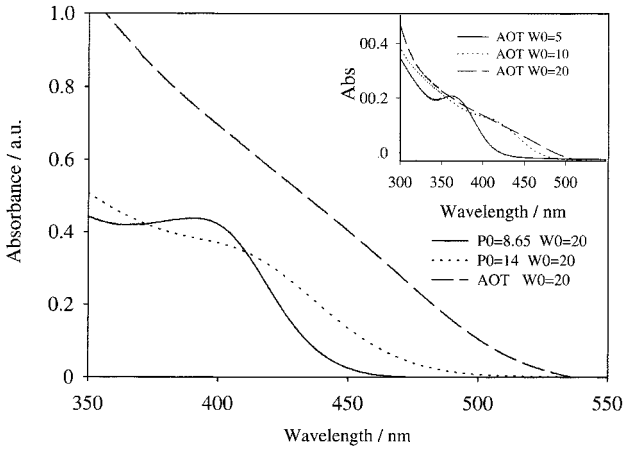

Figure 1. Comparison of and CTAB/*n*-pentanol/*n*-hexane/water microemulsions at $W_0 = 20$ and at different cosurfactant content for quaternary system ([CdS] = 10^{-4}M). In the inset, the absorption spectra of CdS in AOT/isooctane/water at different W_0 are reported.

Synthesis of CdS Nanoparticles. CdS nanoparticles were synthesized in the CTAB microemulsion according to the following procedure: two micellar solutions, at given P_0 and W_0, containing cadmium and sulfide salts, respectively, were prepared. Colloidal CdS particles were then formed by rapidly mixing equal volumes of the two solutions. The same protocol was followed for the preparation of CdS in the AOT microemulsion.

Nucleation occurs immediately after mixing. In CTAB, due to the high exchange dynamic of the micelles, the particles growth is very fast. No substantial change was in fact observed with time in the absorption spectrum (as far as stopped flow experiments were not concerned), as opposed to the evolution in color (in time scale of seconds) experienced when mixing the two AOT solutions of precursors.

A stabilization treatment could be carried out at this stage by addition of thiols (such as dodecanethiol or thiophenol) that act as surface capping agents.

Optical Characterization. Synthesis of cadmium sulfide nanocrystals was monitored by UV−vis absorption spectroscopy. The spectra showed evidence of the quantum confinement effect, indicating the formation of nanometer size particles (Figure 1). Theoretical works[28−31] show that the threshold wavelength of the UV−vis absorption spectrum provides a reasonable estimate of the particle size. From the absorption onset a mean particles size ranging from to 20 to 65 Å (according to the different preparation conditions) could be estimated. The position and the height of the main shoulder in the absorption spectrum are both well related to the size of the semiconductor particles. A third feature of the absorption spectrum is represented by the difference between the position of the onset and the mean position of the shoulder. Because both onset and mean position of the shoulder are related to particle size, their difference provides an estimate of the size polydispersity of the system.

The mean size of semiconductor particles seems to be poorly correlated with the aqueous droplet dimension in the microemulsion (Fig 2), whereas it seems to be dependent on the alcohol content, as the particles dimension increases when P_0 increases.

This experimental evidence is apparently in contrast with the conclusion inferred from the analysis of the spectra of nanosized CdS prepared in a well characterised ternary water-in-oil system (e.g., water/AOT/isooctane) and reproduced in our laboratory (Figure 1, inset). The strong dependence of the onset and peak

position on the W_0 indicates that the particles' growth in that system is governed by the dimensions of the droplets' water core. However, it should be stressed that in a ternary AOT microemulsion, the available range of the water pool radii is wider than the range experienced in the quaternary CTAB microemulsion. For instance, by varying the W_0 from 10 to 30 in AOT microemulsions, an increase of 35 Å in the droplets' radii is observed, whereas a corresponding increase of only 10 Å is observed at $P_0 = 8,6$ in CTAB, this value becoming even smaller at higher P_0 (Figure 2). This different behavior is mainly due to the different properties of the surfactants and to the presence of the co-surfactant, which affects the strong interaction between the charged surfactant polar heads. In a ternary microemulsion such as water/AOT/isooctane, the amphiphilic film that forms the droplet interface has a high rigidity. The water content of the system ultimately dictates the diameter of the water cores. It is not surprising that the control over the nanocrystal's diameter is simply and successfully achieved through variation of the water content. In the CTAB system, the presence of the co-surfactant in the interfacial film greatly affects the microstructure of the droplets; the alkyl tail of the pentanol increases the interfacial curvature by increasing the surfactant packing parameter, thus favoring the formation of small droplets with low water content. This effect is particularly relevant at high pentanol content. Although a complete phase diagram for this quaternary microemulsion is, so far, not available, some comparison can be made with pseudoternary phase diagrams of similar systems. Usually, at high water and surfactant contents, the L2 region contracts to smaller water/surfactant ratio. In this case, the addition of water to the microemulsion has a less remarkable effect on the diameter of the droplets; it mainly leads to the formation of more, small, droplets,[32] until no more surfactant is available for the building up of new micelles and a phase separation occurs. Higher additions of water could be tolerated only by the concomitant addition of surfactant, that is, by shifting to a smaller water/surfactant ratio of the phase diagram.

The curves of Figure 2 also show that the mean size of the droplets in the microemulsion does not always represents an upper limit to the size of the semiconductor particles formed. For instance, particles produced at $P_0 = 14$ are larger than the initial water droplets if the W_0 value is lower than 30. These findings, together with the dependence of the nanoparticles diameters on P_0, are in accordance with previous results concerning the preparation of silica nanoparticles in microemulsions using block copolymers and nonionic surfactants.[33] In particular, the authors studied the addition of different alcohols as cosurfactants. The size of the particles could be controlled by varying the length of the alcohol chain and its concentration; in particular, larger particles were obtained by using both shorter chain and/or higher concentrations. The particles were usually larger than the original water droplets.

The dependence of the particle's radius on the alcohol content can be easily related to the well-known role of the co-surfactant as an agent that increases the interface dynamics of the droplets. Higher pentanol contents favor exchange dynamics and lead to larger particles, even larger than the original droplet diameter.

Moreover, droplets sizes can increase in the presence of salts, as previously reported in literature,[34] as an effect of an increased film flexibility and of a direct interaction between the surfactant and the particles by surface absorption.

Early studies[34] report that the exchange of reactants between water pools should be considered as a reason for size polydispersity. Alcohols are known to reduce the rigidity of the water-in-oil interface and are generally considered responsible for increasing the exchange rates of micelles, thus allowing exchange of solubilized matter and, consequently, Ostwald ripening. The role of the pentanol in influencing particles size and polydispersity is well supported by the analysis of the spectra shown in Figure 1, relative to samples prepared at different composition of the interfacial film, that evidence as an increase of the P_0 results in the shift of absorption onset towards longer wavelengths and in a less structured peak.

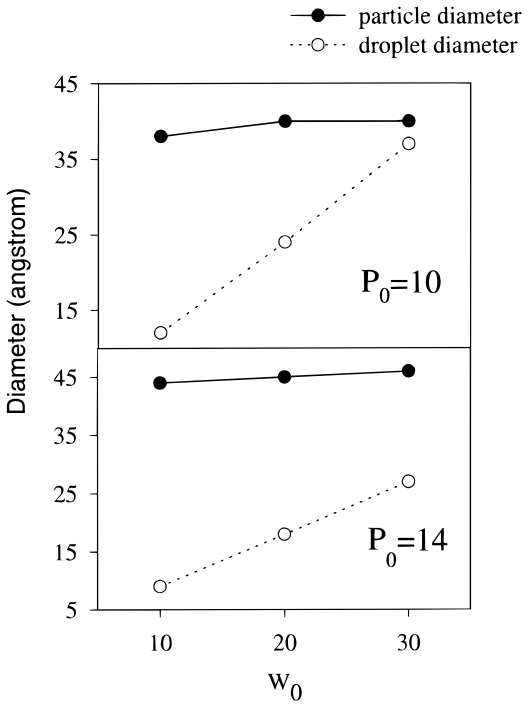

Figure 2. Diagram showing trends in the mean sizes of the droplets and CdS particle in the quaternary CTAB microemulsion as a function of W_0, at $P_0 = 10$ and $P_0 = 14$, respectively.

The intensified activity of the droplet surfaces in the presence of alcohol is evidenced in Figure 3, where the stopped-flow measurements of the CdS formation in the quaternary CTAB and in the ternary AOT microemulsion at the same value of W_0 are reported. The CdS absorption growth in AOT shows a sigmoidal behavior with a lag time of about 50 ms. No evidence of such a delay in the particles formation is shown by the curve relative to the CTAB, whose double exponential behavior clearly evidences the presence of a fast ($t = 10$ms) process of nucleation followed by the crystal growth ($t = 130$ ms).

Moreover, the data reported in Figures 2 and 3 show that, at the same W_0, the water droplets are smaller in a quaternary CTAB microemulsion than in AOT, whereas a lower exchange of the solubilized caused by the compactness of the interface is expected as well as a smallest particles formation. A strong role of the cosurfactant in regulating the growth of the particles by absorption on their surface has indeed to be invoked. Accordingly, the data reported in Figure 4 show that the major role played by pentanol is related to the stability of nanoparticles in solution, as the tendency of the particles to sediment increases when the amount of alcohol in the micellar interface decreases.

The absorption spectra of CdS prepared in microemulsions (at the same W_0 and at two different P_0) recorded immediately after the particles formation, are reported in Figure 4A. The spectra of the same specimens, recorded 24 h later, are shown in the part B of the same figure. Remarkably, a dramatic decrease of the optical intensity of the solution at $P_0 = 8.65$ can be observed, clearly related to the sedimentation of larger

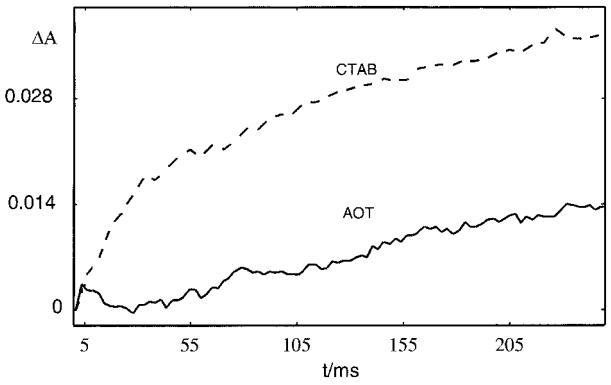

Figure 3. Transient for CdS formation monitored by using stopped flow technique at 400 nm in the AOT ternary system at $W_0 = 20$ (solid line) and at 370 nm in the CTAB quaternary system at $W_0 = 20$, $P_0 = 8.65$ (dotted line).

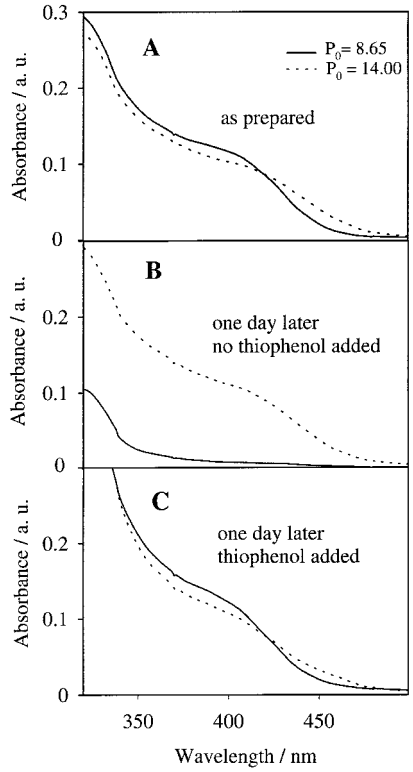

Figure 4. Absorption spectra of CdS in microemulsions at $W_0 = 10$ and at different P_0 values ($P_0 = 8.65$ and $P_0 = 14$, respectively) ([CdS] $= 10^{-4}$ M) (A) as prepared, (B) 1 day later without thiophenol added, and (C) 1 day later with thiophenol added.

crystals, which form a yellow precipitate on the bottom of the cuvette. Conversely, no temporal evolution of the spectrum relative to a solution at $P_0 = 14$ was detected, a surprising result owing to the larger size of the particles. A surface treatment with thiophenol prevents the sample at $P_0 = 8.65$ from precipitation, keeping the nanocrystals in solution and leaves substantially unchanged the spectrum relative to the solution at higher P_0 (Figure 4C).

As a whole, the above-reported results suggest the existence of strong interaction between the cosurfactant and the surface of the particles; at high concentrations, the pentanol behaves as capping agent. This result is somehow unexpected because there is no evidence in the literature of complexes (even weak) between alcohols and cadmium and sulfur atoms.

Nanocrystals were extracted from the micelles according to different procedures: In the first procedure, the microemulsion

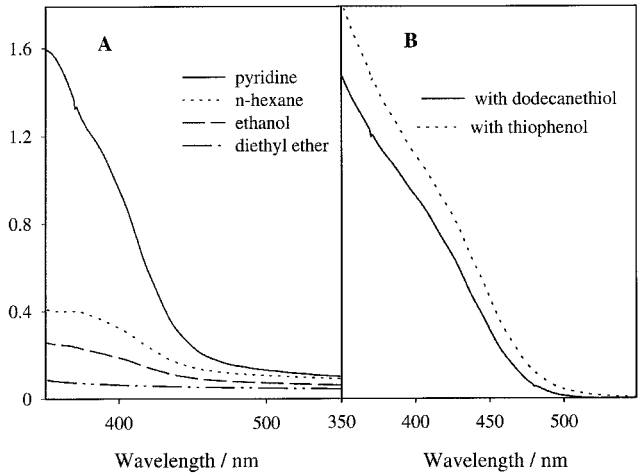

Figure 5. (A) Absorption spectra of CdS nanoparticles after recovery process with thiophenol in a different solvent. (B) Absorption spectra of CdS nanoparticles in pyridine, after recovery process: (a) with thiophenol treatment; (b) with dodecanethiol treatment. Inset: spectra of CdS particles without any capping treatment, after their formation in micellar solution ($P_0 = 14$, $W_0 = 10$, [CdS] $= 10^{-4}$ M).

was evaporated to dryness at 60 °C under vacuum, and the solid was dispersed in ethanol. Centrifugation of this suspension allowed separation of a pale yellow powder that was washed with ethanol and with water. The nanocrystals could then be redissolved in pyridine. The existence of a remarkable absorption of the alcohol on the semiconductor particles is further confirmed by the consideration that the presence of residual pentanol makes the nanocrystals soluble in ethanol, giving a clear yellow solution from which nanoparticles cannot be separated by centrifugation.

Alternatively, organic capping agents such as thiophenol were introduced after the synthesis. A small amount of pyridine was then added. As a consequence of this treatment, the ultrafine particles, temporarily aggregated, were collected and centrifuged. The nanocrystallites were then redissolved in pyridine. The pyridine was chosen as the redispersion agent, in view of its higher capability of solubilization of the CdS particles compared to other organic solvents (see Figure 5A). An evaluation of the effects of different kind of thiols in CdS nanoparticles recovery and redispersibility in solvents was also performed.

CdS in microemulsion treated with thiophenol and dodecanethiol, respectively, was extracted according to the previously described procedure and then redispersed in pyridine. In both cases, the spectra (Figure 5B) provide evidences of a fairly good redispersibility. Moreover, in the region of absorption onset, such spectra are almost identical to those of CdS in microemulsion, providing evidence that the mean diameter and the distribution of CdS particles remain unchanged throughout the redispersion treatment.

The spectrum of thiophenol capped CdS dispersed in pyridine reveals a higher optical density compared to that shown by particles capped with dodecanethiol, confirming an improved efficiency of the former as surface modifier agent. This effect can be reasonably attributed to the stronger acidity of thiophenol, which makes the interactions between Cd ions in excess on nanoparticles surface and thiolate groups more effective.[35−36]

In Figure 6, the UV−vis absorption spectra and the photoluminescence (PL) spectra of two nanocrystallite solutions prepared at two different value of P_0 are finally reported. Again, the absorption spectra show the noticeable shift of the absorption onset between the two samples, indicative of the capability of modulating nanoclusters dimensions by varying P_0.

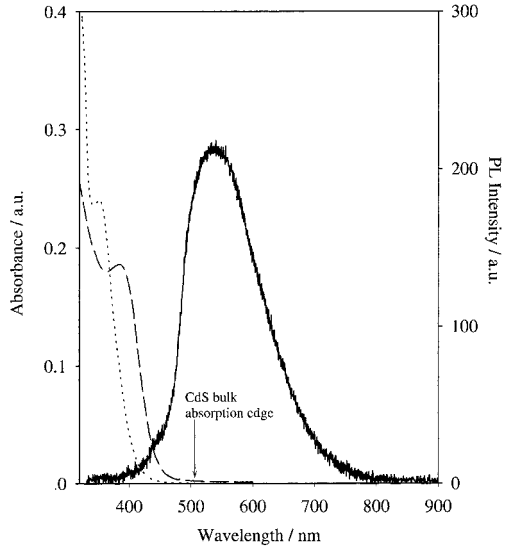

Figure 6. Absorption spectra of CdS nanoparticles microemulsion at $W_0 = 30$ and at different P_0 values ($P_0 = 8.65$ dotted line and $P_0 = 14$ dashed line). The luminescence spectrum (solid line) of CdS nanoparticles sample obtained at $W_0 = 30$ and at $P_0 = 8.65$ (overlapping to the spectrum of CdS sample at $P_0 = 14$ and at the same W_0 value) is also shown. The arrow points out the CdS bulk absorption edge.

The PL bands are shifted to significantly lower energies, and their peak positions do not depend on the different preparative conditions of the two samples. Such a large difference in the spectral positions of absorption and PL and the nondependence of the PL spectrum on particle size does not allow the assignment of the latter to the free or bound exciton luminescence but rather to radiative recombination originated from impurities and surface states.[37]

Raman Analysis. Raman spectroscopy has emerged as a suitable probe for the study of cluster assembled and nanostructured materials.[38−41] The phonon band appearing in the first-order Raman spectrum of a macroscopic crystal has a Lorentzian line shape peaked at $\omega(\boldsymbol{q} = 0)$ phonon frequency. If the crystal size is smaller than about 30 nm, the localization of the phonon wave function causes the relaxation of the $\boldsymbol{q} = 0$ selection rule. Moreover, the enhancement of the surface-to-volume ratio allows observation of the surface phonon mode.[42−43] All of the phonons of the first Brillouin zone can thus take part in the first-order Raman scattering. Raman intensity may then be taken as a weighted sum over all Lorentzian contributions

$$\mathrm{I}(\omega) = \int_{?}^{?} \frac{|C(0, \boldsymbol{q})^2|}{[\omega - \omega(\boldsymbol{q})]^2 + \left(\frac{\Gamma_0}{2}\right)^2} \qquad (1)$$

where the integration is extended to the whole Brillouin zone, $\omega(\boldsymbol{q})$ is the phonon dispersion curve, Γ_0 is the *RT* natural line width, and $C(0,\boldsymbol{q})$ are the Fourier coefficients of the phonon confinement function; using the Gaussian confinement function, proposed by Campbell and Fauchet,[43] $C(0,\boldsymbol{q})$ can be written as

$$|C(0, \boldsymbol{q})^2| = \exp\left(-\frac{\boldsymbol{q}^2 d^2}{16\pi}\right) \qquad (2)$$

where d is the crystallite diameter. We assume an isotropic dispersion curve and a spherical Brillouin zone. These assumptions are justified because only a small region of the Brillouin zone, centered at the Γ point, effectively takes part in the scattering. Using a linear chain model, the LO phonon dispersion

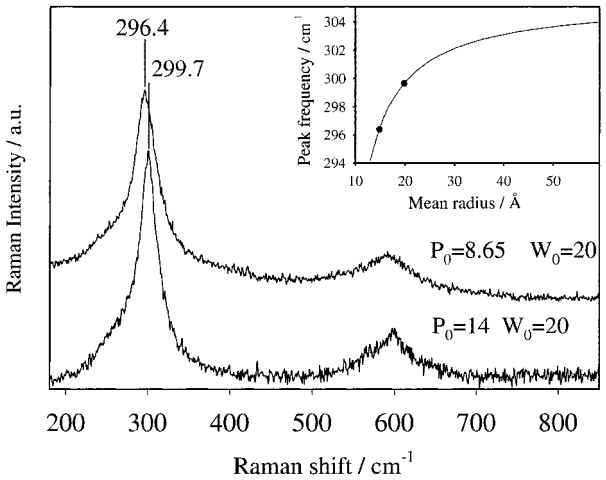

Figure 7. Raman spectra of $P_0 = 8.65$ $W_0 = 20$ and $P_0 = 14$ $W_0 = 20$ samples excited at room temperature with the 4579 Å laser line. In the inset are reported the calculated phonon frequency as a function of the CdS crystallite radius.

can be written as

$$\omega(\boldsymbol{q}) = \frac{\omega_0}{\sqrt{2}} \sqrt{1 + \sqrt{1 - B\sin^2\left(\frac{a\boldsymbol{q}}{2}\right)}} \qquad (3)$$

where ω_0 is the zone center frequency, a is the alloy lattice, and B is a constant describing the dispersion. The relaxation of the $\boldsymbol{q} = 0$ selection rule, for materials with a negative phonon dispersion curve, such as CdS, results in a red-shift of the peak position and low-frequency asymmetric broadening of the Raman bands; the smaller the crystal dimensions, the stronger the finite size effects.

In Figure 7, the Raman spectra obtained for samples prepared at different values of alcohol content are reported. Two broad and asymmetric bands are present in each spectrum, the longitudinal optical (LO) CdS phonon mode and its overtone near 605 cm^{-1}.

As the alcohol content increases, a shift toward higher frequency is observed. The red-shift evaluated by the difference between the peak position of the obtained Raman band and the corresponding bulk frequency phonon allows us to determine the dot's mean radius (see the inset of Figure 7). The obtained mean sizes are in good agreement with the radii of the particles obtained by the absorption onset, again indicating the decreasing of the particle's dimension with the decreasing of the P_0 High-Resolution Transmission Electron Microscopy (HR-TEM).

Samples for TEM observations are obtained by depositing a drop of solution on thin carbon support film on copper grids and allowing the solvent to evaporate.

In Figure 8, a HR-TEM picture of CdS clusters obtained for the sample prepared at P_0 = 14 and ω_0 = 20 is reported. The evidenced area shows one of the clusters that exhibits spherical shape. The regular behavior of the lattice fringes inside the cluster suggests that most clusters have good crystalline structure with no defects. The overlapping of clusters in some areas of the image is due to the TEM samples preparation technique.

The inset of Figure 8 reports the selected area diffraction pattern (SADP). The contribution from the crystalline phase is quite weak due to the high dispersion of clusters in the starting solution and to the contribution of the amorphous support carbon film. Nevertheless, the analysis of the diffraction patterns gives lattice spacing compatible with cubic CdS, although the experimental results do not allow discrimination between the

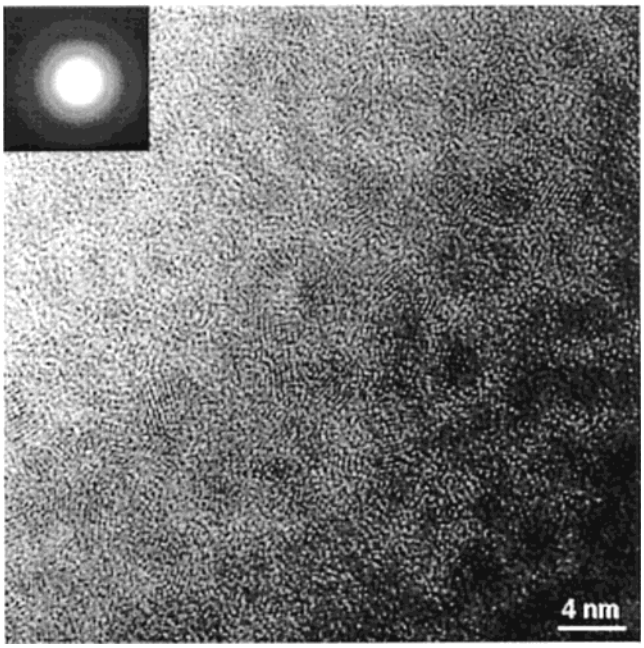

Figure 8. Typical BF HRTEM image from the sample, thiophenol added, prepared at $P_0 = 14$ and $W_0 = 20$. The inset shows the SADP from an area containing several clusters.

cubic and the hexagonal phase because of the overlapping of the diffraction rings. Nanodiffraction experiments are now in progress to try to correctly assess this structural issue.

The statistical analysis of several low-magnification pictures performed on the sample $P_0 = 8.65$; $W_0 = 20$; and $P_0 = 14$; $W_0 = 20$, shows that the clusters have regular shape and narrow size distribution (Figure 9). The diameter size distribution of the particles is peaked around 2.5 ± 0.5 nm for the samples at $P_0 = 8.65$; $W_0 = 20$; and around 3.5 ± 0.5 nm for the $P_0 = 14$, $W_0 = 20$. For both samples, the examined clusters can be grouped in two main families. According to the absorption and Raman data, the particles formed in microemulsion at lower alcohol content are smaller and less disperse compared to those prepared at higher P_0. In particular, the mean radii determined by Raman spectroscopy are slightly greater than those measured by TEM. This discrepancy can be explained if we consider that the Raman efficiency is proportional to the crystallite volume; thus, for the same population, nanocrystals with larger radii give stronger contributions to the scattering.

It is relevant to observe that particles prepared in a ternary AOT microemulsion at the same value of W_0 evidence a much wider distribution of the particles size. The size polydispersity of the particles seems likely related to the droplet size, as at the same water content, the AOT droplets are larger than those formed in the quaternary CTAB emulsion in all of the P_0 range utilized in our measurements. The wider distribution of particle dimensions observed at $P_0 = 14$ seems somehow unexpected in this perspective, as the empty droplets formed at this value of the alcohol content are smaller than those at $P_0 = 8$. Nevertheless, the data reported point out the formation of CdS particles larger than the empty micelles water core, hence suggesting that the volume of the droplets increases in the presence of the semiconductor salt.

Conclusions

The totality of the data obtained using the different techniques indicates, as in the quaternary CTAB microemulsion, that it is possible to prepare small CdS particles characterized by a narrow size distribution and a good degree of crystallinity. A new effective procedure for extracting the particles has been also developed.

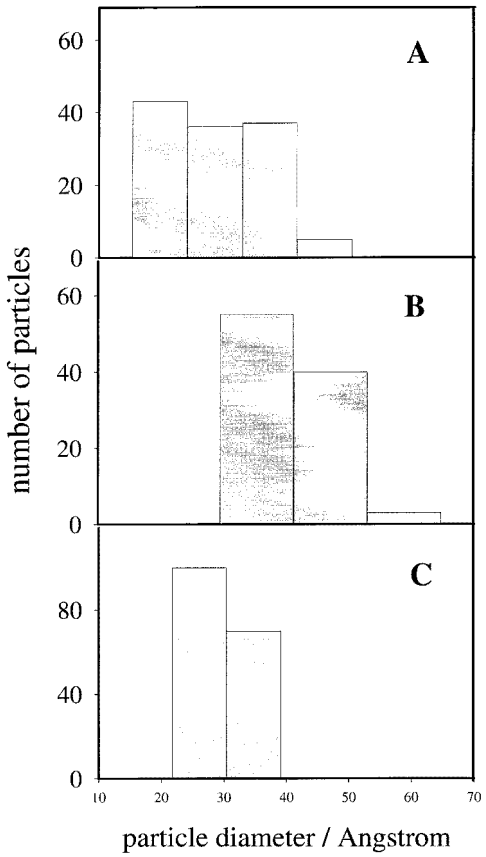

Figure 9. Hystograms showing size distribution of CdS nanoparticles samples obtained from (A) AOT ternary microemulsion at $W_0 = 5$, (B) CTAB quaternary microemulsion at $P_0 = 14$, $W_0 = 20$, (C) CTAB quaternary microemulsion at $P_0 = 8.65$, $W_0 = 20$.

The presence of the alcohol in the microemulsion is concluded to be a key factor in regulating the size, size distribution, and stability of the crystallites. The role played by the pentanol can be summarized in two different actions; from one side, the increased flexibility of the interfacial film influences the particles growth, and from the other side, the absorption on the semiconductor surface determines the particle's stabilization in solution, acting as a capping agent. The possibility of obtaining stable semiconductor nanoparticles in solution without the addition of external capping agents opens interesting perspectives in their use as functional materials in chemical processes or for optoelectronic devices.[44]

Acknowledgment. This work was partially supported by CNR Progetto Finalizzato Biotecnologie. Dr. W. Vastarella is kindly acknowledged for the stopped flow measurements.

References and Notes

(1) Tricot, Y. M.; Fendler, J. H. *J. Am. Chem. Soc.* **1984**, *106*, 7359.
(2) Hagfeldt, A.; Gratzel, M. *Chem. Rev.* **1995**, *95*, 49.
(3) Meyer, M.; Wallberg, C.; Kurihara, K.; Fendler, J. *J. Chem. Soc. Chem. Commun.* **1984**, 90.
(4) Khaleel, A.; Li, W. F.; Klabunde, K. J. *Nanostructur. Mater.* **1999**, *12*, 463.
(5) Clark, D.; Wood, D.; Erb, U. *Nanostruct. Mater.* **1997**, *9*, 755.
(6) Bach, U.; Lupo, D.; Comte, P.; Moser, J. E.; et al. *Nature* **1998**, *395*, 583.
(7) Colvin, V. L.; Schlamps, M. C.; Alivisatos, A. P.*Nature* **1994**, *370*, 354.

(8) Klein, D. L.; Roth, R.; Lim, A. K. L.; et al. *Nature* **1997**, *389*, 699.
(9) Takahashi, N.; Ishikuro, H.; Hiramoto, T. *Appl. Phys. Lett.* **2000**, *76*, 209.
(10) Bruchez, M.; Moronne, M.; Gin, P.; Weiss, S.; et al. *Science* **1998**, *281*, 2013.
(11) Loweth, C. J.; Caldwell, W. B.; Peng, X. G.; Alivisatos, A. P.; et al. *Angew. Chem.-Int. Ed. Engl.* **1999**, *38*, 1808.
(12) Kortan, A. R.; Hull, R.; Opila, R. L.; Bawendi, M. G.; Steigerwald, M. L.; Carrol, P. J.; Brus, L. E. *J. Am. Chem. Soc.* **1990**, *112*, 1327.
(13) Eastoe, J.; Warne, J. B. *Curr. Opin. Colloid. Interface Sci.* **1996**, *1*, 800.
(14) Alivisatos, A. P. *Science* **1996**, *271*, 933.
(15) Murray, C. B.; Norris, D. J.; Bawendi, M. G. *J. Am. Chem. Soc.* **1993**, *115*, 8706.
(16) Sato, H.; Hirai, T.; Komasawa, I. *Ind. Eng. Chem. Res.* **1995**, *34*, 2493.
(17) Petit, C.; Jain, T. K.; Billoudet, F.; Pileni, M. P. *Langmuir* **1994**, *10*, 4446.
(18) Cizeron, J.; Pileni, M. P. *J. Phys. Chem.* **1995**, *99*, 17 410.
(19) Cizeron, J.; Pileni, M. P. *J. Phys. Chem.* **1997**, *101*, 8887.
(20) Pileni, M. P. *Langmuir* **1997**, *13*, 3266.
(21) Tanori, J.; Duxin, N.; Petit, C.; Veillet, P.; Pileni, M. P. *Colloid. Polym. Sci.* **1995**, *273*, 886.
(22) Steigerwald, M. L.; Alivisatos, A. P.; Gibson, J. M.; Harris, T. D.; Kortan, A. R.; Muller, A. J.; Thayer, A. M.; Duncan, T. M.; Douglass, D. C.; Brus, L. E. *J. Am. Chem. Soc.* **1988**, *110*, 3046. Bowen-Katari, J. E.; Colvin, V. L.; Alivisatos, A. P. *J. Phys. Chem.* **1994**, *98*, 4109.
(23) Agostiano, A.; Catalano, M.; Curri, M. L.; Della Monica, M.; Manna, L.; Vasanelli, L. *Micron* **2000**, *31*, 253.
(24) Tian, Y.; Newton, T.; Kotov, N. A.; Guldi, D. M.; Fendler, J. H. *J. Phys. Chem.* **1996**, *100*, 8927.
(25) Shiojiri, S.; Hirai, T.; Komasawa, I. *J. Chem. Eng. Japan* **1997**, *30*, 86.
(26) Giustini, M.; Palazzo, G.; Colafemmina, G., Della Monica, M.; Giomini, M.; Ceglie, A. *J. Phys. Chem.* **1996**, *100*, 3190.
(27) Vossmeyer, T.; Katsikas, L.; Giersig, M.; Popovic, I. G.; Diesner, K.; Chemseddine, A.; Eychmuller A.; Weller, H. *J. Phys. Chem.* **1994**, *98*, 7359.
(28) .Towey, T. F.; Khan-Lodhi, A.; Robinson B. H. *J. Chem. Soc., Faraday Trans.* **1990**, *86*, 3757.
(29) Lianos, P.; Thomas, J. K. *J. Colloid Interface Sci.* **1987**, *117*, 505.
(30) Lianos, P.; Thomas, J. K. *Chem. Phys. Lett.* **1986**, *125*, 299.
(31) Brus, L. E. *J. Chem. Phys.* **1984**, *80*, 4403.
(32) Maidment, L. J.; Chen, V.; Warr, G. G. *Colloids Surf. A* **1997**, *129*−*130*, 311.
(33) Esquena, J.; Tadros, T. F.; Kostarelos, K.; Solans, C. *Langmuir* **1997**, *13*, 6400.
(34) Modes, S.; Lianos, P. *J. Phys. Chem.* **1989**, *93*, 5854.
(35) Murakoshi, K.; Hosokawa, H.; Saito, M.; Yanagida, S. *J. Colloid Interface Sci.* **1998**, *203*, 225.
(36) Nosaka, Y.; Ohta, N.; Fukuyama, T.; Fujii, N. *J. Colloid Interface Sci.* **1993**, *155*, 23.
(37) Artemyev, M. V.; Sperling, V.; Woggon, U. *J. Crystal Growth* **1998**, *184/185*, 374.
(38) Rossetti, R.; Nakahara, S., Brus, L. E. *J. Chem. Phys.* **1983**, *79*, 1086.
(39) Alivisatos, A. P.; Harris, T. D.; Carrol, P. J.; Steigerwald, M. L.; Brus, L. E. *J. Chem. Phys.* **1989**, *90*, 3463.
(40) Scamarcio, G.; Lugarà, M.; Manno, D. *Phys. Rev. B* **1992**, *45*, 13 792.
(41) Spagnolo, V.; Scamarcio, G.; Lugarà, M.; Righini, G. C. *Superlattices Microstruct.* **1994**, *16*, 51.
(42) Richter, H.; Wang, Z. P.; Levy, L. *Solid State Commun.* **1981**, *39*, 625.
(43) Campbell, I. H.; Fauchet, P. M. *Solid State Commun.* **1986**, *58*, 739.
(44) Leo, G.; Curri, M. L.; Cola, A.; Catalano, M.; Lomascolo, M.; Manna, L.; Quaranta, F.; Agostiano, A.; Farinola, G. M.; Babudri, F.; Naso, F.; Della Monica, M.; Vasanelli, L. *Mater. Sci. Eng., B* **2000**, *74*, 175.